Development of Standing-Wave Labyrinthine Patterns[*]

Arik Yochelis[†], Aric Hagberg[‡], Ehud Meron[§], Anna L. Lin[¶], and Harry L. Swinney[¶]

Abstract. Experiments on a quasi-two-dimensional Belousov–Zhabotinsky (BZ) reaction-diffusion system, periodically forced at approximately twice its natural frequency, exhibit resonant labyrinthine patterns that develop through two distinct mechanisms. In both cases, large amplitude labyrinthine patterns form that consist of interpenetrating fingers of frequency-locked regions differing in phase by π. Analysis of a forced complex Ginzburg–Landau equation captures both mechanisms observed for the formation of the labyrinths in the BZ experiments: a transverse instability of front structures and a nucleation of stripes from unlocked oscillations. The labyrinths are found in the experiments and in the model at a similar location in the forcing amplitude and frequency parameter plane.

Key words. labyrinthine patterns, Belousov–Zhabotinsky reaction, complex Ginzburg–Landau equation

AMS subject classifications. 35, 37

PII. S1111111101397111

1. Introduction.
Labyrinthine patterns occur in a variety of equilibrium and nonequilibrium systems. Competition between two interacting phases in diblock copolymers [21], ferrofluids [25], and Langmuir films [25] results in labyrinthine domain patterns of the two phases at equilibrium. Labyrinths made of superconducting and normal phases are found in thin films of type-I superconductors [13]. Nonequilibrium labyrinthine patterns are observed in chemical reaction-diffusion systems with a Turing instability [22] and in bistable reaction-diffusion systems [14, 17]. Although periodically forced oscillatory systems have been studied in the context of traveling waves and spiral waves [2, 1, 26, 8], only a few studies have focused on labyrinthine standing-wave patterns. Labyrinthine patterns have been found in numerical simulations of the periodically forced Brusselator reaction-diffusion equations [18] and in numerical solutions of the normal form equation for the oscillation amplitude [1, 23].

Experiments on the periodically forced photosensitive Belousov–Zhabotinsky (BZ) reaction produce nonequilibrium labyrinthine patterns when the system is forced with time-

periodic pulses of light that are approximately twice the system's natural oscillation frequency [24, 18]. In this case, the two phases correspond to two phases of oscillation, each locked to the time-periodic forcing and shifted by π with respect to one another. We observe that the standing-wave labyrinthine patterns form in two distinct ways: from a transverse instability of planar fronts connecting the two phase-locked states or by nucleating stripes from unlocked oscillating domains. Even though the mechanisms are different, the resulting patterns in both cases are large amplitude labyrinths.

In this paper, we explain the experimental observations using a normal form equation for periodically forced oscillatory systems. We demonstrate the two mechanisms for labyrinthine pattern formation and give criteria for the parameter regions where they act. Since the mechanisms of labyrinthine pattern formation are found in a normal form equation, these mechanisms should also be observed in other periodically forced oscillatory systems such as electro-convection [15].

2. Experimental results. We create chemical labyrinths in a porous membrane (0.4 mm thick, 22 mm diameter) fed by two reservoirs. Each reservoir contains a subset of the chemical reactants for the oscillatory photosensitive (ruthenium catalyzed) BZ reaction [18, 24], and the two reservoirs are in contact with opposite faces of the porous membrane. We force the reaction externally with spatially homogeneous time-periodic square waves of light. The patterns form in the membrane as variations in the concentration of the chemical catalyst Ru(III). The unforced pattern is a rotating spiral wave of Ru(III) concentration. Parametric forcing with light modulated in intensity at a frequency that is approximately twice that of the chemical oscillation frequency results in chemical patterns that oscillate once every two forcing cycles. These patterns, which we call 2:1 resonant patterns, consist of synchronous domains that oscillate with a relative phase difference of π.

Photobleaching experiments [19] reveal that the membrane supports spatially uniform oscillations over a range of chemical concentrations. We conduct our experiments within this range; thus our experimental conditions are far from the Hopf bifurcation. The labyrinthine patterns we describe here are 2:1 resonant with the natural frequency (the spatially homogeneous oscillation frequency), not the oscillation frequency of the spiral pattern [18].

Different resonant patterns are observed, depending on the forcing frequency ω_f and the forcing strength γ [18]. The region of 2:1 resonant dynamics forms a tongue in the $\omega_f - \gamma$ parameter space [12]. For most parameter values in the tongue, the patterns consist of irregularly shaped standing-wave domains differing in phase by π. Near the bottom of the tongue, there are rotating phase-locked spiral waves, and, on one side of the tongue, standing-wave labyrinthine patterns form [18], as shown in Figure 1. Outside the range of 2:1 resonant dynamics, patterns are either unlocked or locked at a different resonance.

A useful way to characterize the spatio-temporal patterns is in terms of the complex Fourier amplitude $a(x, y)$ of a particular mode in the time series of each pixel (x, y) in the pattern [18]. We look at $a(x, y)$ for the $\omega_f/2$ mode, the primary response mode of the pattern. For each pixel (x, y) in the labyrinthine pattern of Figure 1, $a(x, y)$ is plotted as a black dot in the Re-Im plane shown in Figure 2(a). The points located at the ends of the "S"-shaped curve correspond to pixels in one of the two phase-locked domains. The other points are from the interfaces between domains. The ends of the "S"-shaped curve are π out of phase, which
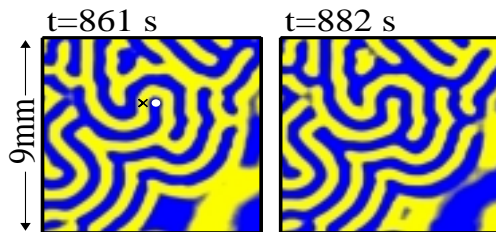
Labyrinthine pattern observed in the BZ reaction (pattern sampled every 2 seconds) [movie] [27].
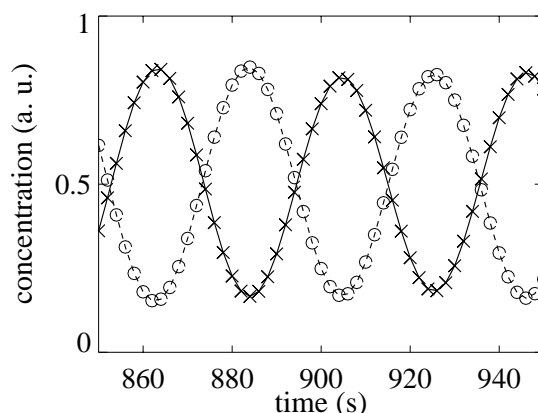

Figure 1. *Resonant labyrinthine pattern in the* 2:1 *periodically forced BZ reaction. (top) The two images show the spatial* Ru(III) *concentration pattern in a* 9 *mm region of the chemical reactor. Yellow represents regions of high* Ru(III) *concentration, and blue represents regions of low concentration. The images are at two different times separated by one forcing period (*21 *s). (bottom) A time series from two locations in the top pattern (marked with "x" and "∘") shows that the pattern is formed of regions of two different phases separated by* π. *The chemical conditions are given in Figure* 3.

shows that the phase-shift between the yellow and the blue domains pictured in Figure 1 is π. The distribution of points in Figure 2(a) as a function of phase angle $\theta = \arg(a(x, y))$ is shown in Figure 2(b). The histogram shows that most of the pattern is in one of the two phase-locked states, $\theta = 0$ and $\theta = \pi$, which correspond to the yellow and blue regions in Figure 1. From this representation of the data, we clearly see that the observed labyrinths are large amplitude patterns comprised of two phase-locked, π-shifted domains, as opposed to small amplitude modulations on one or both of the two phases.

The development of labyrinthine patterns by the two mechanisms is shown in Figure 3. A labyrinth can grow from a transverse instability of a front that separates two phase-locked domains, as shown in Figure 3(a). A labyrinth pattern can also develop, stripe by stripe, from an unlocked oscillatory state, as shown in Figure 3(b). The resulting labyrinthine pattern in Figure 3(b) is similar to the labyrinth shown in Figure 3(a); both patterns consist of standing-wave domains oscillating with a relative phase-shift of π.
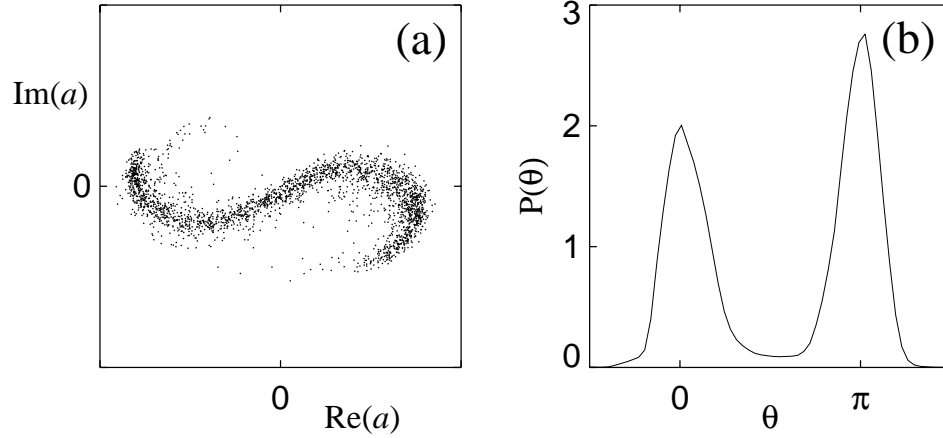
Figure 2. (a) *The complex Fourier amplitude $a(x, y)$ of the $\omega_f/2$ mode corresponding to the labyrinthine pattern shown in Figure* 1, *plotted in the* Re-Im *phase plane.* (b) *A histogram $P(\theta)$ of the phase angle $\theta = \arg(a)$. Most of the pattern is locked at one of two phase angles, $\theta = 0, \pi$.*

3. Theoretical analysis. To study the mechanisms by which these chemical labyrinths form, we model the oscillating BZ chemical reaction as an extended system with a Hopf bifurcation to uniform oscillations. Let **u** be a vector field of chemical concentrations responding at $\omega_f/2 \approx \omega_0$, where ω_0 is the frequency of the unforced system and ω_f is the forcing frequency. Near a supercritical Hopf bifurcation, the field can be written as

$$(3.1) \qquad \mathbf{u} = \mathbf{u_0} A e^{i\omega_f t/2} + \text{complex conjugate } (c.c.) + \cdots,$$

where $\mathbf{u_0}$ is a constant, A is a complex amplitude, and the ellipses denote higher order terms. The amplitude of oscillation $A(x, y, \tau)$ is slowly varying in space and time and is described by the complex Ginzburg–Landau equation [11, 1, 6, 7]

$$(3.2) \qquad A_\tau = (\mu + i\nu)A + (1 + i\alpha)\nabla^2 A - (1 + i\beta)|A|^2 A + \gamma A^*.$$

The equation has been scaled to its reduced form, where μ is the distance from the Hopf bifurcation, ν is the detuning (the deviation of ω_f from $2\omega_0$), α is a dispersion parameter, and γ is the forcing amplitude. The term A^* is the complex conjugate of A and appears from the addition of 2:1 periodic forcing [11]. To simplify the following discussion, we set $\beta = 0$.

When $\mu > 0$, the spatially uniform solution $A = 0$ is unstable. In the unforced system ($\gamma = 0$), (3.2) has a continuous family of uniformly oscillating solutions

$$(3.3) \qquad A = \sqrt{\mu} e^{i\nu\tau + i\phi_0},$$

where ϕ_0 is an arbitrary constant phase. Equation (3.2) also has plane wave solutions, but we do not consider them here. The existence of a continuous family of solutions when $\gamma = 0$ is a consequence of the phase-shift invariance of (3.2), $A \to A\exp(i\phi_0)$, which follows from the time translation symmetry of the unforced oscillatory system. The forcing term γA^* restricts the phase-shift invariance to π phase-shifts. At $\gamma = |\nu|$, two stable uniform phase-locked
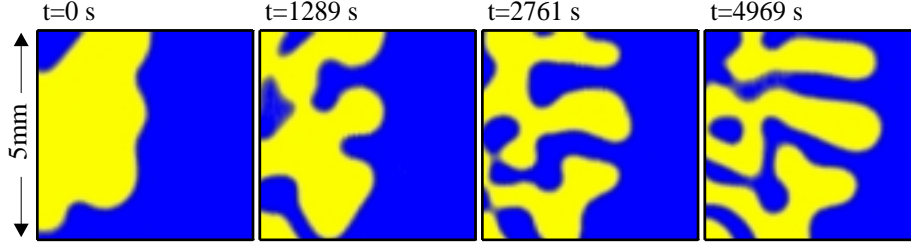
Labyrinthine pattern formation by transverse front instability (strobed at the pattern frequency) [movie] [27].
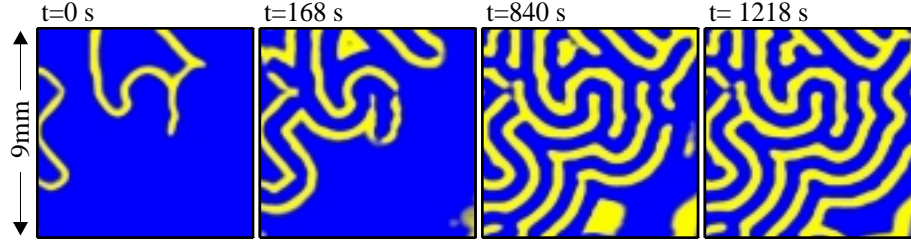
Labyrinthine pattern formation by nucleation of stripes (strobed at the pattern frequency) [movie] [27].

Figure 3. *Formation of labyrinthine patterns through (top) a transverse front instability and (bottom) a nucleation of stripes. The patterns are from a region of the BZ reactor, strobed at half the forcing frequency. Blue (yellow) represents regions of low (high)* Ru(III) *concentration. (a) $\gamma = 600$ W/m^2, $\omega_f = 0.273$ rad/s. Reservoir* I: 0.22 *M malonic acid,* 0.046 *M* KBr0$_3$, 0.2 *M* KBr, *and* 0.8 *M* H$_2$SO$_4$; *reservoir* II: 1.0 *mM* Ru(2, 2' − bipyridine)$_3$ + 2, 0.8 *M* H$_2$SO$_4$, *and* 0.184 *M* KBrO$_3$. *The flow rates through each reservoir are* 20 *ml/h and* 5 *ml/h, respectively. The reservoir volumes are each* 10 *ml. (b)* $\gamma = 228$ W/m^2, $\omega_f = 0.300$ *rad/s. Reservoir* I: 0.22 *M malonic acid,* 0.2 *M* NaBr, 0.264 *M* KBrO$_3$, 0.8 *M* H$_2$SO$_4$; *reservoir* II: 0.184 *M* KBrO$_3$, 1×10^{-3} *M Tris(2, 2'-bipyridyl)dichlororuthenium*(II)*hexahydrate,* 0.8 *M* H$_2$SO$_4$. *The volume of each reservoir was* 8.3 *ml. The flow rate through reservoir* I *was* 20 *ml/h; that through reservoir* II *was* 5 *ml/h.*

solutions are formed in a pair of saddle-node bifurcations on a circle of amplitude $|A|$. These solutions describe oscillations at precisely half the forcing frequency, $\omega_f/2$, even though for $\nu \neq 0$ the oscillation frequency of the unforced system differs from $\omega_f/2$. The phases of the two solutions differ by π.

To see how these solutions appear, we consider spatially uniform solutions of (3.2) and write the complex amplitude in a polar form, $A = |A| \exp{(i\phi)}$. Using this form in (3.2), we find

(3.4)
$$\phi_\tau = \nu - \gamma \sin(2\phi) \,.$$

In order for (3.1) to describe resonant dynamics, we must look for stationary solutions of (3.4) (so that **u** oscillates at $\omega_f/2$). Stationary solutions of this equation exist for $\gamma \geq |\nu|$:

(3.5)
$$\phi_S^- = \frac{1}{2} \arcsin\left(\frac{\nu}{\gamma}\right) \,, \qquad \phi_S^+ = \phi_S^- + \pi \,,$$
$$\phi_U^- = \frac{\pi}{2} - \frac{1}{2} \arcsin\left(\frac{\nu}{\gamma}\right) \,, \qquad \phi_U^+ = \phi_U^- + \pi \,,$$

where the subscripts S and U refer to stable and unstable solutions, respectively. At $\gamma = |\nu|$,

the two pairs of solutions, ϕ_S^-, ϕ_U^- and ϕ_S^+, ϕ_U^+ are born in saddle-node bifurcations, as shown in Figure 4(a). The condition $\gamma > |\nu|$ defines the 2:1 resonance tongue, where the system's frequency is locked to one half of the forcing frequency. The resonance tongue in the ν-γ plane is shown in Figure 4(b).
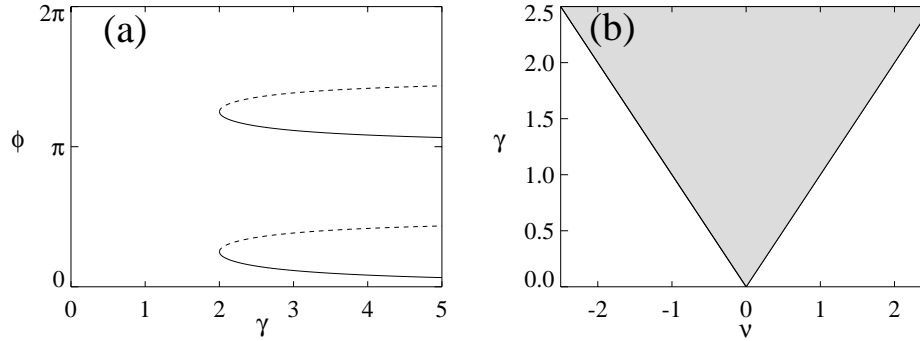

Figure 4. (a) *Bifurcation diagrams showing the formation of the four stationary phase solutions in* (3.5) *for fixed detuning ($\nu = 2$) and varying forcing strength γ. The solid (dashed) curves represent stable (unstable) solutions.* (b) *The existence range of the phase solutions in* (a), $\gamma > |\nu|$, *defines the resonance tongue in the ν-γ plane (shaded region) inside which the original system responds at half the forcing frequency.*

Inside the tongue, front structures form between the two phases ϕ_S^- and ϕ_S^+. At low forcing γ, the fronts travel, and the domains organize into two-phase spiral waves [1, 9]. As the forcing is increased, the system goes through a nonequilibrium Ising–Bloch (NIB) bifurcation [2, 8]. For $\nu = \alpha = 0$, the NIB bifurcation point is at $\gamma = \mu/3$. A numerically computed NIB bifurcation boundary for nonzero ν and α values is shown in Figure 5(a). Above the NIB bifurcation, only stationary Ising fronts exist. In the following, we confine ourselves to the Ising regime well beyond the NIB bifurcation.

When $\alpha \neq 0$, there is a range of parameters in the $\nu - \gamma$ parameter plane where the Ising fronts are unstable to transverse perturbations. The boundary of this linear transverse instability can be computed numerically and is shown as the line γ_T in Figure 5(b).

When $\gamma > \gamma_T$, the fronts are stable, and domains of the two phases persist for long periods. For $\nu < \gamma < \gamma_T$, stationary fronts are unstable. Perturbations along the front grow into fingers, which tip, split, and form labyrinthine patterns, as shown in Figure 6(a). The amplitude of the labyrinth approaches that of the uniform phase-locked states $|A| \sim (\mu + \sqrt{\gamma^2 - \nu^2})^{1/2}$ and is large because of the large distance μ from the Hopf bifurcation. Note the similarity to the experimental labyrinth formation shown in Figure 3(a).

Outside the tongue ($\gamma < \nu$), uniform phase-locked solutions do not exist, but resonant labyrinthine patterns still persist [23]. The labyrinthine patterns form in a range $\gamma_N < \gamma < \nu$ outside the tongue boundary and, similar to the labyrinths inside the tongue, are characterized by large amplitudes. This observation can be explained by a coupling of a finite-wavenumber (Turing) mode to a zero-wavenumber mode [5, 20, 3]. In the present case, the zero-wavenumber mode has uniform oscillations. In the following, we derive equations for the amplitudes of these modes and use them to obtain a criterion for the boundary γ_N.

Consider the dispersion relation associated with perturbations, $A \sim \exp(\sigma\tau - ikx)$, of the
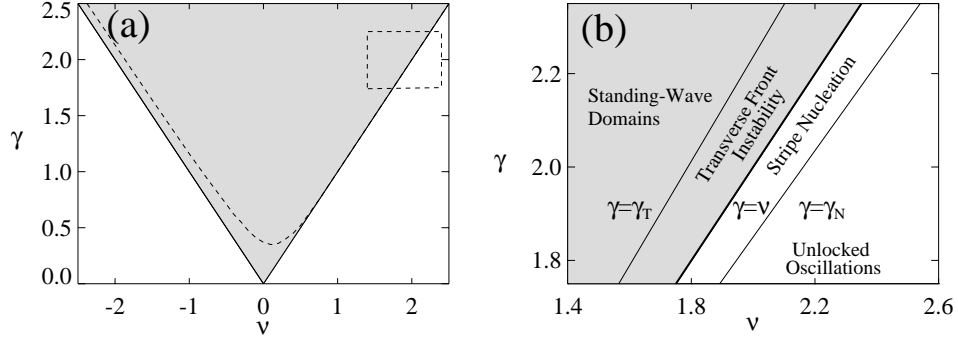
Figure 5. (a) *The NIB bifurcation boundary (dashed curve) inside the resonance tongue, obtained by numerical integration of* (3.2). *Below the boundary, the fronts that connect the two stable phase-locked states, ϕ_S^- and ϕ_S^+, are traveling Bloch fronts. Above the boundary, the fronts are stationary Ising fronts.* (b) *A closeup of the rectangular region indicated in* (a) *showing the regions where a labyrinthine pattern forms. For $\nu < \gamma < \gamma_T$, a labyrinth forms by a transverse front instability, while, for $\gamma_N < \gamma < \nu$, it forms by stripe nucleation from the unlocked oscillating state. Outside these regions, the dominant pattern is unlocked oscillations ($\gamma < \gamma_N$) or irregularly shaped standing-wave domains with nearly stationary interfaces ($\gamma > \gamma_T$). The boundaries γ_N and γ_T are computed from direct numerical solution of* (3.2). *Parameters: $\mu = 1$, $\beta = 0$, $\alpha = 0.5$.*

$A = 0$ state

(3.6)
$$\sigma(k) = \mu - k^2 + \sqrt{\gamma^2 - (\nu - \alpha k^2)^2}.$$

At the codimension 2 point, $\mu = 0$, $\gamma = \gamma_c$, where

$$\gamma_c = \frac{\nu}{\sqrt{1 + \alpha^2}},$$

two modes become marginally stable in a Turing–Hopf bifurcation [16, 4]. That is, the growth rates, shown in Figure 7, are zero for both a zero-k mode describing uniform oscillations, $k = 0$, $\omega = \omega_0$, and a finite-k mode describing a stationary pattern, $k = k_c$, $\omega = 0$, where $\omega = \text{Im}(\sigma)$ and

$$k_c^2 = \frac{\nu\alpha}{1 + \alpha^2},$$
$$\omega_0 = \frac{\nu\alpha}{\sqrt{1 + \alpha^2}}.$$

To study the coupling of the two modes, we assume $|\mu| \sim |d| \ll 1$, where $d := \gamma - \gamma_c$, and we consider (3.2) in one space dimension. We then express A in terms of its real and imaginary parts, $A = U + iV$, and expand

(3.7)
$$\begin{pmatrix} U \\ V \end{pmatrix} = \sqrt{\mu} \begin{pmatrix} U_0 \\ V_0 \end{pmatrix} + \mu \begin{pmatrix} U_1 \\ V_1 \end{pmatrix} + \mu^{3/2} \begin{pmatrix} U_2 \\ V_2 \end{pmatrix} + \cdots,$$

where the ellipses denote higher order contributions and

(3.8)
$$\begin{pmatrix} U_0 \\ V_0 \end{pmatrix} = \mathbf{e_0} B_0 (X, T) e^{i\omega_0 \tau} + \mathbf{e_k} B_k (X, T) e^{ik_c x} + c.c.$$
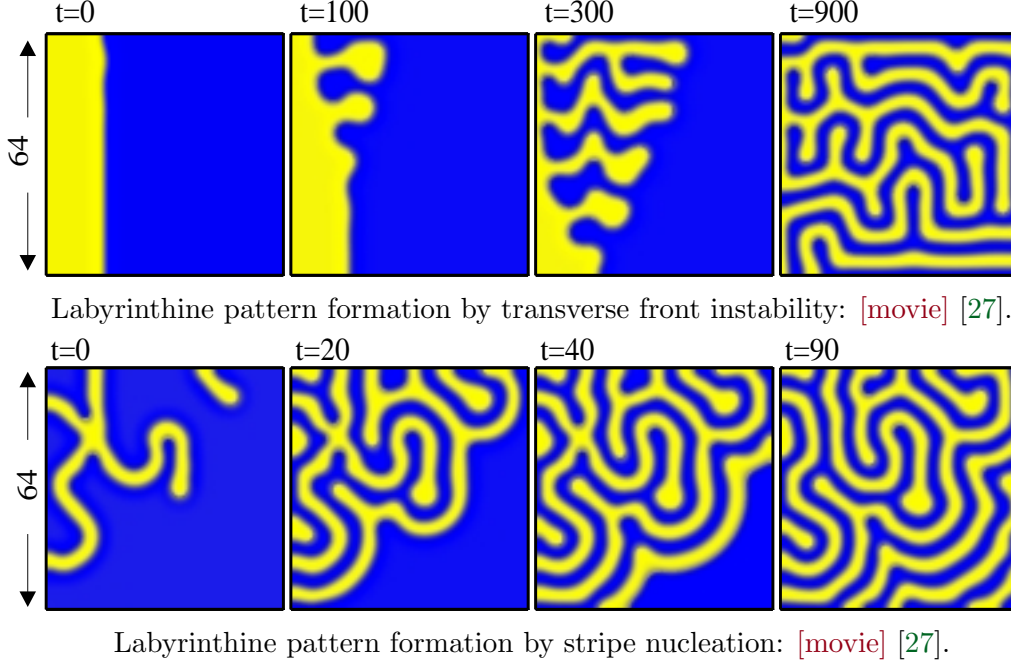
Labyrinthine pattern formation by transverse front instability: [movie] [27].

Labyrinthine pattern formation by stripe nucleation: [movie] [27].

Figure 6.   *Formation of labyrinthine patterns in* (3.2). *Blue and yellow regions are different phases separated by* π. *(top) When* $\nu < \gamma < \gamma_T$ *(*$\gamma = 2.02$*), the interface between the phase-locked domains is transversely unstable, and small perturbations grow and finger. (bottom) Outside the tongue, when* $\gamma_N < \gamma < \nu$ *(*$\gamma = 1.98$*), the pattern forms by nucleating stripes from the unlocked oscillating state. The stripes are unstable to the zigzag instability. Other parameters:* $\mu = 1$, $\nu = 2.0$, $\alpha = 0.5$.

Here $\mathbf{e_0}$ and $\mathbf{e_k}$ are the eigenvectors corresponding to the eigenvalues $\sigma(0)$ and $\sigma(k_c)$, respectively.

The amplitudes B_0 and B_k in (3.8) describe weak spatio-temporal modulations of the (relatively) fast oscillations associated with the zero-k mode and of the strong spatial variations associated with the finite-k mode. The weak dependence is expressed by the introduction of the slow variables $T = \mu\tau$, $X = \sqrt{\mu}x$.

Inserting the expansion (3.7) into (3.2), solving the linear equations at order μ, and evaluating the solvability condition at order $\mu^{3/2}$, we find the amplitude equations

$$\partial_T B_0 = (\mu - i\zeta)B_0 - 4\left|B_0\right|^2 B_0 - (a - ib)\left|B_k\right|^2 B_0 + (1 + i\rho)\partial_X^2 B_0\,,$$

(3.9) $$\partial_T B_k = \eta B_k - c_1\left|B_k\right|^2 B_k - 8\left|B_0\right|^2 B_k + c_2\partial_X^2 B_k\,,$$

with the coefficients

$$
\begin{aligned}
\zeta &= d/\alpha \quad (d = \gamma - \gamma_c)\,,\\
\eta &= \mu + \zeta\rho\,,\\
\rho &= \sqrt{1 + \alpha^2}\,,\\
a &= 8\rho(\rho + \alpha)\,,\\
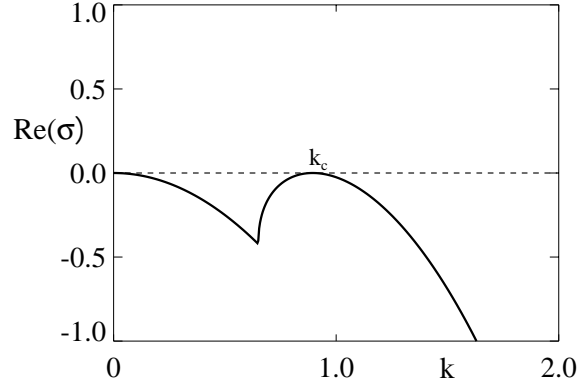b &= 4(\rho + \alpha)\,,
\end{aligned}
$$

Figure 7. *The growth rate $\mathrm{Re}(\sigma)$ for perturbations of the $A = 0$ solution at the codimension 2 point: $\mu = 0$, $\gamma = \gamma_c$. Two modes become marginal at this point: a zero-k (Hopf) mode and a finite-k (Turing) mode. Parameters: $\mu = 0$, $\nu = 2.0$, $\alpha = 0.5$, $\gamma = \gamma_c \approx 1.8$.*

$$c_1 = 3a/4 \,,$$
$$c_2 = 2\rho^2 \,.$$

More details about the derivation of (3.9) will be presented elsewhere.

Equations (3.9) have two families of pure-mode uniform solutions,

(3.10)
$$B_0 = \frac{1}{2}\sqrt{\mu}e^{-i\zeta T + i\psi_1} \,, \qquad B_k = 0 \,,$$

representing uniform oscillations, and

(3.11)
$$B_0 = 0 \,, \qquad B_k = \sqrt{\eta/c_1}e^{i\psi_2} \,,$$

representing stationary periodic patterns, where ψ_1 and ψ_2 are arbitrary constants. Outside and close enough to the tongue boundary ($\gamma = \nu$), both families of solutions are linearly stable. The family of solutions representing stationary patterns, however, loses stability as γ is decreased past

(3.12)
$$\gamma_S = \gamma_c - \frac{\mu\alpha}{4\sqrt{1 + \alpha^2}} = \frac{\nu - \mu\alpha/4}{\sqrt{1 + \alpha^2}} \,.$$

Figure 8 shows the boundary $\gamma = \gamma_S$ as computed from (3.12) and compared with results from the direct numerical solution of (3.2) in one space dimension. The agreement is good despite the relatively large value of μ.

The amplitude equations (3.9) also have a mixed-mode family of uniform solutions ($B_0 \neq 0$, $B_k \neq 0$), but these solutions are unstable.

The existence boundary of resonant stripes $\gamma = \gamma_S$ is well below the boundary $\gamma = \gamma_N$, where stripes are observed to nucleate from the unlocked oscillation state. This observation can be understood by considering front solutions of (3.9) which are biasymptotic to the two states $(0, B_k)$ and $(B_0, 0)$ as $x \to \pm\infty$. Numerical studies of these equations in the range
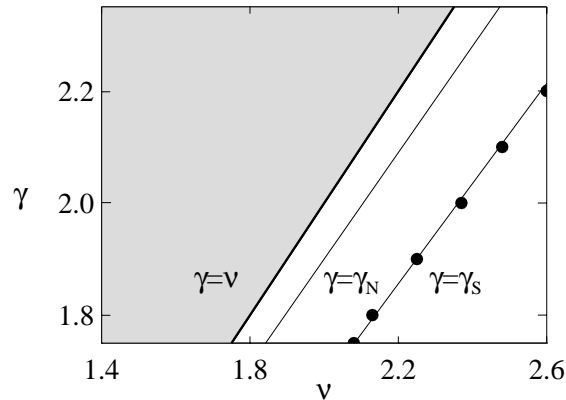
Figure 8. *The boundaries γ_S of stationary stripe patterns and γ_N of stripe nucleation outside of the resonance tongue. The line $\gamma = \gamma_S$ was computed using (3.12), and the solid circles represent the numerical solution of the model equation (3.2). The line $\gamma = \gamma_N$ was computed by direct numerical solution of (3.9). Stationary stripes are stable between the tongue boundary $\gamma = \nu$ and γ_S but nucleate from unlocked oscillations only between $\gamma = \nu$ and γ_N. When $\gamma < \gamma_S$, the stripes are unstable to uniform oscillations. The parameter values are the same as in Figure 5.*

$\gamma_S < \gamma < \nu$ show the existence of a zero front-velocity line. We identify this line with the boundary $\gamma = \gamma_N$. For $\gamma > \gamma_N$, the stationary stripe state, $(0, B_k)$, invades the uniform oscillation state, $(B_0, 0)$, and in this sense is dominant. In the context of (3.2), this invasion takes the form of stripe nucleation, as Figure 6(b) shows. The stripes nucleate stripe by stripe at the boundary of the growing stationary pattern domain. The stripes are also unstable to transverse perturbations (zigzag instability). Note the similarity to the experimental labyrinth formation shown in Figure 3(b).

The analysis of the amplitude equations (3.9) also provides the amplitude of the stationary stripes. The amplitude of the stripes is given by $|B_k| = \sqrt{\eta/c_1}$ (see (3.11)). Far from the Hopf bifurcation where $\mu \sim O(1)$, $|B_k|$ can be of order unity even at $\gamma = \gamma_N$. This explains the large amplitude values of the stationary stripe patterns in the range $\gamma_N < \gamma < \nu$.

4. Conclusions. Both the experiments and the complex Ginzburg–Landau equation produce nonequilibrium labyrinthine patterns through two different mechanisms: a transverse instability of fronts between locked states and a nucleation of stripes from an unlocked oscillating state. Unlike previous studies of phase-locked labyrinthine patterns, the labyrinths are not small amplitude patterns modulating one of the phase-locked states [1]. Resonant labyrinths persist even outside the 2:1 tongue of uniform phase-locked states in the complex Ginzburg–Landau model, indicating that the boundary for resonant patterns in extended oscillating systems need not coincide with that of a single forced oscillator. The large amplitude of the labyrinths both inside and outside the tongue boundary is a consequence of the large distance of the system from the Hopf bifurcation.

The labyrinthine patterns are found on only one side of the 2:1 resonance tongue both in the experiments and in the forced complex Ginzburg–Landau equation. In the experiments, they are found on the side of the tongue closest to the 3:1 resonance tongue. In (3.2), the side

of the tongue is determined by the sign of the parameter α.

Similar labyrinthine patterns have been observed in numerical solutions of the forced Brusselator reaction-diffusion system [18] but without a description of the underlying mechanism. Those results show similar features, such as the labyrinths forming in a region on only one side of the resonance tongue. Since the complex Ginzburg–Landau equation we study is a generic model, we expect to find the same mechanisms for labyrinthine pattern formation in other 2:1 resonant oscillatory systems.

Quantitative comparison between the experiment and the model is difficult because the chemical kinetics and diffusion coefficients are not well known. The parameter values in a complex Ginzburg–Landau model depend on these quantities. The two mechanisms of labyrinthine pattern formation are also expected to be found in liquid crystal systems with dynamics described by (3.2) [10, 9].

REFERENCES

[1] P. COULLET AND K. EMILSSON, *Strong resonances of spatially distributed oscillators: A laboratory to study patterns and defects*, Phys. D, 61 (1992), pp. 119–131.

[2] P. COULLET, J. LEGA, B. HOUCHMANZADEH, AND J. LAJZEROWICZ, *Breaking chirality in nonequilibrium systems*, Phys. Rev. Lett., 65 (1990), pp. 1352–1355.

[3] A. DE WIT, *Spatial patterns and spatiotemporal dynamics in chemical systems*, Advances in Chemical Physics, 109 (1999), pp. 435–513.

[4] A. DE WIT, D. LIMA, G. DEWEL, AND P. BORCKMANS, *Spatiotemporal dyanmics near a codimension-two point*, Phys. Rev. E (3), 54 (1996), pp. 261–271.

[5] G. DEWEL, S. MÉTENS, M. HILALI, P. BORCKMANS, AND C. B. PRICE, *Resonant patterns through coupling with a zero mode*, Phys. Rev. Lett., 74 (1995), pp. 4647–4650.

[6] C. ELPHICK, A. HAGBERG, AND E. MERON, *A phase front instability in periodically forced oscillatory systems*, Phys. Rev. Lett., 80 (1998), pp. 5007–5010.

[7] C. ELPHICK, A. HAGBERG, AND E. MERON, *Multiphase patterns in periodically forced oscillatory systems*, Phys. Rev. E (3), 59 (1999), pp. 5285–5291.

[8] C. ELPHICK, A. HAGBERG, E. MERON, AND B. MALOMED, *On the origin of traveling pulses in bistable systems*, Phys. Lett. A, 230 (1997), pp. 33–37.

[9] T. FRISCH AND J. M. GILLI, *Excitability and defect-mediated turbulence in nematic liquid crystal*, J. Phys. II France, 5 (1995), pp. 561–572.

[10] T. FRISCH, S. RICA, P. COULLET, AND J. M. GILLI, *Spiral waves in liquid crystal*, Phys. Rev. Lett., 72 (1994), pp. 1471–1474.

[11] J. M. GAMBAUDO, *Perturbation of a Hopf-bifurcation by an external time-periodic forcing*, J. Differential Equations, 57 (1985), pp. 172–199.

[12] J. A. GLAZIER AND A. LIBCHABER, *Quasi-periodicity and dynamical systems: An experimentalist's view*, IEEE Trans. Circuits Systems, 35 (1988), pp. 790–809.

[13] F. HAENSSLER AND L. RINDERER, *Statique et dynamique de l'état intermédiaire des supraconducteurs du type I*, Helv. Phys. Acta, 40 (1967), pp. 659–687.

[14] A. HAGBERG AND E. MERON, *From labyrinthine patterns to spiral turbulence*, Phys. Rev. Lett., 72 (1994), pp. 2494–2497.

[15] T. KAWAGISHI, T. MIZUGUCHI, AND M. SANO, *Points, walls, and loops in resonant oscillatory media*, Phys. Rev. Lett., 75 (1995), pp. 3768–3771.

[16] H. KIDACHI, *On mode interactions in reaction diffusion equation with nearly degenerate bifurcations*, Progr. Theoret. Phys., 63 (1980), pp. 1152–1169.

[17] K. J. Lee and H. L. Swinney, *Lammelar structures and self-replicating spots in a reaction-diffusion system*, Phys. Rev. E (3), 51 (1995), pp. 1899–1915.

[18] A. L. Lin, M. Bertram, K. Martinez, H. L. Swinney, A. Ardelea, and G. F. Carey, *Resonant phase patterns in a reaction-diffusion system*, Phys. Rev. Lett., 84 (2000), pp. 4240–4243.

[19] K. Martinez, A. L. Lin, R. Kharrazian, X. Sailer, and H. L. Swinney, *Resonance in periodically inhibited reaction-diffusion systems*, Phys. D, 2 (2002), pp. 168–169.

[20] S. Métens, G. Dewel, P. Borckmans, and R. Engelhardt, *Pattern selection in bistable systems*, Europhys. Lett., 37 (1997), pp. 109–114.

[21] G. E. Molau, ed., *Colloidal and Morphological Behavior of Block and Graft Copolymers*, Plenum Press, New York, 1971.

[22] Q. Ouyang and H. L. Swinney, *Transition from a uniform state to hexagonal and striped Turing patterns*, Nature (London), 352 (1991), pp. 610–612.

[23] H.-K. Park, *Frequency locking in spatially extended systems*, Phys. Rev. Lett., 86 (2001), pp. 1130–1133.

[24] V. Petrov, Q. Ouyang, and H. L. Swinney, *Resonant pattern formation in a chemical system*, Nature, 388 (1997), pp. 655–657.

[25] M. Seul and D. Andelman, *Domain shapes and patterns: The phenomenology of modulated phases*, Science, 267 (1995), pp. 476–483.

[26] D. Walgraef, *Spatio-Temporal Pattern Formation*, Springer-Verlag, New York, 1997.

[27] Additional movie formats available at http://math.lanl.gov/Labyrinth/.